

## Interaction between Na and Li in ZnO

Pekka T. Neuvonen,<sup>1,a)</sup> Lasse Vines,<sup>1</sup> Andrej Yu. Kuznetsov,<sup>1</sup> Bengt G. Svensson,<sup>1</sup> Xiaolong Du,<sup>1,b)</sup> Filip Tuomisto,<sup>2</sup> and Anders Hallén<sup>3</sup>

<sup>1</sup>Department of Physics, Centre for Material Science and Nanotechnology, University of Oslo, P.O. Box 1048 Blindern, N-0316 Oslo, Norway

<sup>2</sup>Department of Applied Physics, Helsinki University of Technology, P.O. Box 1100, 02015 TKK Espoo, Finland

<sup>3</sup>Department of Microelectronics and Applied Physics, Royal Institute of Technology, School of ICT, P.O. Box Electrum 229, SE-164 40 Kista, Sweden

(Received 29 October 2009; accepted 10 November 2009; published online 16 December 2009)

The interaction between group-Ia elements in ZnO have been studied by implanting Na into hydrothermally grown ZnO samples containing  $\sim 4 \times 10^{17}$  Li/cm<sup>3</sup> and employing secondary ion mass spectrometry for sample analysis. Postimplantation annealing above 500 °C results in a diffusion of Na and concurrently Li is efficiently depleted from the regions occupied by Na. The data show unambiguously that Na and Li compete for the same trapping site and the results provide strong experimental evidence for that the formation energies of Na on Zn site together with that of interstitial Li are lower than those of Li on Zn site and interstitial Na in highly resistive ZnO. This conclusion is also supported by recent theoretical estimates of the formation energies of these species as a function of the Fermi-level position in ZnO. © 2009 American Institute of Physics. [doi:10.1063/1.3270107]

Zinc oxide (ZnO) is a wide and direct band-gap ( $E_g \approx 3.34$  eV) semiconductor with high exciton binding energy ( $\sim 60$  meV).<sup>1</sup> These properties make it highly desirable for optoelectronic applications,<sup>2,3</sup> such as light-emitting diodes, lasers, etc. Furthermore, recent developments in ZnO growth methods<sup>4,5</sup> have made high quality single crystal ZnO wafers available with the capability to scale up wafer size. However, mastering of reliable *p*-type doping remains, in spite of decade-long research efforts/expectations, a major obstacle for device implementation in ZnO. Indeed, as-grown ZnO typically exhibits *n*-type conductivity which is often explained in terms of intrinsic defects—oxygen vacancy ( $V_O$ ) and zinc interstitial ( $Zn_i$ )<sup>6–8</sup>—or impurities incorporated during the growth, such as hydrogen<sup>9,10</sup> and/or metallic impurities (Al, In, etc.).<sup>11,12</sup> However, none of these can alone account for the native *n*-type behavior of ZnO,<sup>13</sup> and the effect may be explained in terms of a combination of contributions from different possible donorlike defects and impurities in ZnO. In contrast, there are fundamental challenges to form reasonably stable and shallow enough acceptor levels with sufficient concentration to provide reliable *p*-type ZnO. Hence, there is a fierce and on-going effort worldwide—both by theoretical and experimental means—addressing the acceptor development in ZnO.<sup>14</sup>

Based on theoretical predictions<sup>15</sup> and preliminary experimental data,<sup>16</sup> group-Ia elements, specifically, Li and Na, may potentially act as shallow acceptors when incorporated on Zn site— $Li_{Zn}$  and  $Na_{Zn}$ . The results from Refs. 15 and 16 are, however, controversial since other studies suggest that  $Na_{Zn}$  exhibit a deep acceptor level ( $\sim 0.6$ – $0.8$  eV above the valence band edge).<sup>17</sup> Further, an overall drawback is that  $Li_{Zn}$  ( $Na_{Zn}$ ) acceptors may readily convert into donorlike de-

fects where the Li(Na) atoms occupy interstitial sites,  $Li_i$  ( $Na_i$ ). Specifically, calculations show that the donorlike configurations are becoming more energetically favorable with decreasing Fermi-level ( $E_F$ ) position explained in terms of low ionization energy of *s* electrons and matrix size mismatch with group-Ia ions.<sup>14</sup> However, experimentally the knowledge is scarce about stability of these different atomic configurations and this holds especially for the interplay between group-Ia elements (e.g., Li and Na) competing for similar sites in the ZnO lattice.

In this work, we apply secondary ion mass spectrometry (SIMS) to study the interaction between Li and Na in ZnO. Highly resistive hydrothermally (HT) grown samples ( $\rho \sim 10$  kΩ cm) containing  $\sim 4 \times 10^{17}$  Li/cm<sup>3</sup>, have been implanted with 150 keV Na<sup>+</sup> using a dose of  $1 \times 10^{15}$  cm<sup>-2</sup>. Control samples were implanted with 150 keV Ne<sup>+</sup> ions producing similar amount of energy deposition into elastic and ionizing collisions as Na<sup>+</sup>. Both the Na<sup>+</sup> and Ne<sup>+</sup> ion implants were performed at room temperature using a 7° tilt angle of the samples to reduce channeling effects, resulting in a projected range of  $\sim 230$  nm. Subsequently, the samples were annealed in air at 450, 500, and 550 °C for 60, 60, and 30 min, respectively.

Li and Na concentration versus depth profiles were measured by SIMS after all processing steps with Cameca IMS7f microanalyzer. 10 keV O<sub>2</sub><sup>+</sup> ions were used as a primary beam rastered over a surface area of  $125 \times 125$  μm<sup>2</sup> and secondary ions (<sup>7</sup>Li<sup>+</sup>, <sup>23</sup>Na<sup>+</sup>, <sup>70</sup>Zn<sup>+</sup>) were collected from the central part of the craters with detection limit in the low  $10^{14}$  cm<sup>-3</sup> range for both Li and Na. Crater depths were measured with a Dektak 8 stylus profilometer, and the erosion rate was assumed to be constant when converting sputtering time to sample depth. Li and Na concentration calibrations were performed using implanted reference samples.

Figure 1 shows Na (lines) and Li (lines with symbols), concentration profiles after postimplant annealing at different temperatures. Note that no diffusion (of neither Li nor Na) is

<sup>a)</sup>Electronic mail: p.t.neuvonen@smn.uio.no.

<sup>b)</sup>Permanent address: Institute of Physics, The Chinese Academy of Sciences, Beijing 100190, People's Republic of China.

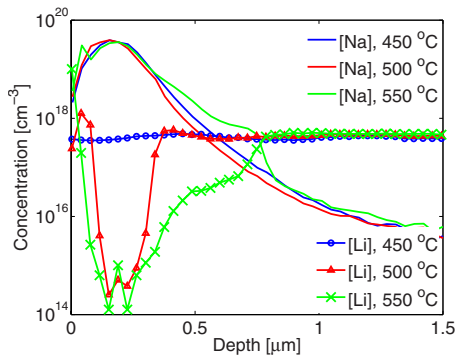


FIG. 1. (Color online) Na (lines) and Li (lines with symbols) concentrations vs depth profiles in Na implanted samples after different anneals. Note that symbols are for eye guidance only and the actual profiles contain more experimental points.

observed after annealing at 450 °C so that both the Li and Na profiles are identical to the as-implanted ones (not shown). However, increasing the temperature to 500 °C causes a dramatic change in the Li profile within the implanted region—strong depletion of Li from the depth corresponding to the maximum concentration of the Na profile—while the Na concentration profile itself remains practically unchanged. A further increase in the temperature up to 550 °C results in a measurable Na diffusion and concurrently, Li is depleted from exactly the same part of the sample that is becoming occupied by Na atoms, including the Na diffusion tail (0.4–0.8 μm in Fig. 1) where the concentration of implantation-induced defects is substantially lower than in the peak region. These results show a strong interaction between Li and Na, which can be attributed to a competition between the two elements for some trapping sites in the lattice; the results also suggest that there is a maximum concentration limit of Li and Na combined which the samples can accommodate under equilibrium conditions.

It is known that intrinsic defects and defect complexes may be responsible for Li redistribution in ZnO during postimplantation annealing too, typically reported to occur at temperatures  $\geq 600$  °C.<sup>18</sup> Hence, the evolution observed in Fig. 1 may be alternatively explained in terms of interaction of group-Ia dopants with implantation-induced defects and a “control” measurement is decisive. Figure 2 shows the Li concentration versus depth profiles from Ne implanted control samples. No dramatic changes (neglecting some redistribution in the vicinity of the surface) are detected in the Li

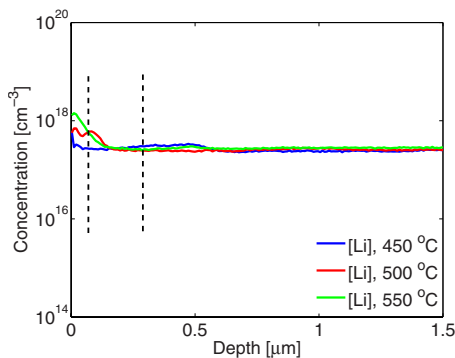


FIG. 2. (Color online) Li concentration vs depth profiles in Ne implanted samples after different anneals. Dashed lines indicate the implantation peak region.

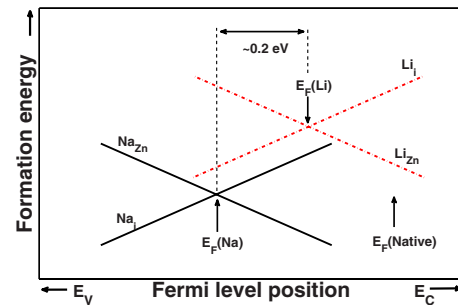


FIG. 3. (Color online) Schematics of formation energies of  $\text{Li}_{\text{Zn}}$ ,  $\text{Li}_i$ ,  $\text{Na}_{\text{Zn}}$ , and  $\text{Na}_i$  vs Fermi-level position in ZnO after Ref. 21. The Fermi-levels are pinned to  $E_F$  (native),  $E_F$  (Li) and  $E_F$  (Na) in undoped, Li-rich, and Na-rich ZnO, respectively, as indicated by arrows.

profiles after any of the annealing steps (Fig. 2). This excludes unambiguously that implantation-induced (intrinsic) defects only are responsible for the Li redistribution observed in Fig. 1

The high resistivity of the HT ZnO wafers used indicate that Li acts as acceptor<sup>19</sup> predominantly residing on zinc site. On the other hand, the implanted Na is probably randomly distributed existing in different configurations, e.g., clusters and precipitates, of limited temperature stability. In this context, it can be pointed out that results from Rutherford backscattering spectrometry (RBS) measurements reveal that the implanted layer is not heavily damaged showing a concentration of displaced Zn atoms below the detection limit ( $< 10^{20}$  cm<sup>-3</sup>). The results presented in Fig. 1 suggest that at  $\sim 500$  °C, Na is likely to become mobile, presumably through release of trapped  $\text{Na}_i$ , and changing its configuration to predominantly  $\text{Na}_{\text{Zn}}$ , which is energetically more favorable than  $\text{Li}_{\text{Zn}}$ . In other words,  $E_{\text{form}}(\text{Na}_{\text{Zn}}) + E_{\text{form}}(\text{Li}_i) < E_{\text{form}}(\text{Na}_i) + E_{\text{form}}(\text{Li}_{\text{Zn}})$ , in which  $E_{\text{form}}$  is the formation energy of the defect. Consequently, all substitutional traps are filled with Na and  $\text{Li}_i$  will diffuse out of the region. Interestingly, the scanning spreading resistance microscopy (SSRM) profiling of the Na implanted and annealed samples (not shown) confirms that the resistivity is not decreasing in spite of the out-diffusion of Li supporting the hypothesis of  $\text{Li}_{\text{Zn}}$  to  $\text{Na}_{\text{Zn}}$  acceptor exchange in the samples upon annealing. Moreover, PAS results<sup>20</sup> indicate no increase in open volume associated with Zn vacancies but rather a decrease which is consistent with a  $\text{Na}_{\text{Zn}}$  configuration occupying efficiently the zinc vacancy.

A strong support of the suggested scenario for the Na–Li interplay in ZnO is provided by considering defect formation energy variations as a function of  $E_F$ , as predicted by theory, and Fig. 3 is a schematics of that for  $\text{Li}_i$ ,  $\text{Li}_{\text{Zn}}$ ,  $\text{Na}_i$ , and  $\text{Na}_{\text{Zn}}$  in ZnO, based on calculations performed by Wardle *et al.*<sup>21</sup> They concluded that both Li and Na would prefer residing on interstitial sites at low (*p*-type) values of  $E_F$  while substitutional sites are preferable at high (*n*-type) values of  $E_F$ . In its native form, as discussed in the introduction, ZnO exhibits generally *n*-type conductivity and  $E_F$  is close to the conduction band edge ( $E_C$ ). However, if Li is present, as in our HT-samples—it will predominantly appear in the  $\text{Li}_{\text{Zn}}$  acceptor-like form resulting in an increase in resistivity and lowering of the  $E_F$  position, which is ultimately pinned at  $E_F(\text{Li})$ , as labeled in Fig. 3, if the Li concentration is sufficiently high. According to Ref. 21,  $E_F(\text{Li}) > E_g/2$  explaining the difficulty to achieve *p*-type ZnO with Li doping. Importantly,

Na behaves similarly to Li, with the Fermi-level pinning point [ $E_F(\text{Na})$  in the Fig. 3] possibly shifted by  $\sim 0.2$  eV toward lower energies.<sup>21</sup> If  $\text{Na}_i$  is introduced into a material where  $\text{Li}_{\text{Zn}}$  dominates, an inevitable conclusion from Fig. 3 is that under equilibrium conditions  $\text{Na}_i$  and  $\text{Li}_{\text{Zn}}$  exchange configurations to  $\text{Na}_{\text{Zn}}$  and  $\text{Li}_i$  since  $[E_{\text{form}}(\text{Na}_{\text{Zn}}) + E_{\text{form}}(\text{Li}_i)] < [E_{\text{form}}(\text{Na}_i) + E_{\text{form}}(\text{Li}_{\text{Zn}})]$ . As a result, Li becomes highly mobile, via the interstitial configuration, and diffuses rapidly out of the Na-rich region since the trapping sites ( $V_{\text{Zn}}$ ) are occupied by Na. In fact, the rapid out-diffusion of Li is further enhanced if  $E_F < E_F(\text{Li})$  in the Na-rich regions, which is a distinct possibility according to Fig. 3, promoting the formation of  $\text{Li}_i$  relative to that  $\text{Li}_{\text{Zn}}$ .

Finally, the annealing temperature of 500 °C, which is required to start the transformation from  $\text{Li}_{\text{Zn}}$  to  $\text{Na}_{\text{Zn}}$  in our samples, indicates a reaction barrier height of  $\sim 2$  eV, assuming an attempt frequency of  $\sim 10^{13}$  s<sup>-1</sup>. This reaction barrier is possibly determined by the release of  $\text{Na}_i$  from the implanted region.

In summary, the behavior of group-Ia elements in ZnO have been investigated and a strong interaction between Li and Na is observed at  $\geq 500$  °C. The experimental data demonstrate clearly that Li and Na compete for the same trapping sites and strong evidence is obtained that  $[E_{\text{form}}(\text{Na}_{\text{Zn}}) + E_{\text{form}}(\text{Li}_i)] < [E_{\text{form}}(\text{Na}_i) + E_{\text{form}}(\text{Li}_{\text{Zn}})]$  in highly resistive material. These results are fully consistent with recent theoretical predictions and explain the observed rapid out-diffusion of Li from the Na-rich region.

The authors gratefully acknowledge support from the Norwegian Research Council through the NANOMAT and FRI-NAT programs for the fundings as well as NordForsk grants providing resources for the international collaboration.

- <sup>1</sup>D. G. Thomas, *J. Phys. Chem. Solids* **15**, 86 (1960).
- <sup>2</sup>Y. R. Ryu, T. S. Lee, J. A. Lubguba, H. W. White, Y. S. Park, and C. J. Youn, *Appl. Phys. Lett.* **87**, 153504 (2005).
- <sup>3</sup>A. Tsukazaki, M. Kubota, A. Ohtomo, T. Onuma, K. Ohtani, H. Ohno, S. F. Chichibu, and M. Kawasaki, *Jpn. J. Appl. Phys., Part 2* **44**, L643 (2005).
- <sup>4</sup>K. Maeda, M. Sato, I. Niikura, and T. Fukuda, *Semicond. Sci. Technol.* **20**, S49 (2005).
- <sup>5</sup>D. C. Reynolds, C. W. Litton, D. C. Look, J. E. Hoelscher, B. Claffin, T. C. Collins, J. Nause, and B. Nemeth, *J. Appl. Phys.* **95**, 4802 (2004).
- <sup>6</sup>S. E. Harrison, *Phys. Rev.* **93**, 52 (1954).
- <sup>7</sup>A. R. Hutson, *Phys. Rev.* **108**, 222 (1957).
- <sup>8</sup>A. F. Kohan, G. Ceder, D. Morgan, and C. G. Van de Walle, *Phys. Rev. B* **61**, 15019 (2000).
- <sup>9</sup>S. F. J. Cox, E. A. Davis, S. P. Cottrell, P. J. C. King, J. S. Lord, J. M. Gil, H. V. Alberto, R. C. Vilão, J. Piroto Duarte, N. Ayres de Campos, A. Weidinger, R. L. Lichti, and S. J. C. Irvine, *Phys. Rev. Lett.* **86**, 2601 (2001).
- <sup>10</sup>G. A. Shi, M. Stavola, S. J. Pearton, M. Thieme, E. V. Lavrov, and J. Weber, *Phys. Rev. B* **72**, 195211 (2005).
- <sup>11</sup>R. Schifano, E. V. Monakhov, L. Vines, B. G. Svensson, W. Mtangi, and F. D. Auret, *J. Appl. Phys.* **106**, 043706 (2009).
- <sup>12</sup>E. V. Monakhov, A. Y. Kuznetsov, and B. G. Svensson, *J. Phys. D* **42**, 153001 (2009).
- <sup>13</sup>A. Janotti and C. G. Van de Walle, *Phys. Rev. B* **76**, 165202 (2007).
- <sup>14</sup>Y. Yan and S.-H. Wei, *Phys. Status Solidi B* **245**, 641 (2008).
- <sup>15</sup>C. H. Park, S. B. Zhang, and S.-H. Wei, *Phys. Rev. B* **66**, 073202 (2002).
- <sup>16</sup>S. Lin, J. Lu, Z. Ye, H. He, Z. Gu, L. Chen, J. Huang, and B. Zhao, *Solid State Commun.* **148**, 25 (2008).
- <sup>17</sup>B. K. Meyer, J. Sann, and A. Zeuner, *Synth. Met.* **38**, 344 (2005).
- <sup>18</sup>T. Moe Børseth, F. Tuomisto, J. S. Christensen, W. Skorupa, E. V. Monakhov, B. G. Svensson, and A. Y. Kuznetsov, *Phys. Rev. B* **74**, 161202 (2006).
- <sup>19</sup>B. G. Svensson, T. Moe Børseth, K. M. Johansen, T. Masqood, R. Schifano, U. Grossner, J. Christensen, L. Vines, P. Klason, Q. X. Zhao, M. Willander, F. Tuomisto, W. Skorupa, E. V. Monakhov, and A. Yu. Kuznetsov, *Mat. Res. Soc. Symp. Proc.* **1035**, L04 (2008).
- <sup>20</sup>P. T. Neuvonen *et al.* (unpublished).
- <sup>21</sup>M. G. Wardle, J. P. Goss, and P. R. Briddon, *Phys. Rev. B* **71**, 155205 (2005).